Measurements of the Circular Polarization of Radio Sources at Frequencies of 0·63, 1·4, 5·0 and 8·9 GHz

J. A. Roberts,[A] *R. S. Roger,*[A,B] *J.-C. Ribes,*[A,C] *D. J. Cooke,*[A]
J. D. Murray,[A] *B. F. C. Cooper*[A] *and F. Biraud*[D]

[A] Division of Radiophysics, CSIRO, P.O. Box 76, Epping, N.S.W. 2121.
[B] Present address: Dominion Radio Astrophysical Observatory, Penticton, B.C., Canada.
[C] Present address: Observatoire de Paris, Section d'Astrophysique, Meudon, France.
[D] Observatoire de Paris, Section d'Astrophysique, Meudon, France.

Abstract

Circular polarization measurements were made with the Parkes 64 m telescope on 66 mainly extragalactic sources, 33 of which were studied at two or more frequencies. Circular polarization was definitely found in the eight quasi-stellar sources PKS 0237−23, 0537−441, 1127−14, 1226+02 (3C 273), 1253−05 (3C 279), 2134+004, 2145+06 and 2345−16, as it was measured at the 4σ level or higher in at least two observing sessions. For all eight sources the total power spectrum shows the effects of self-absorption. For none of the eight is there evidence of a reversal of the sense of polarization with frequency. For several of the sources the degree of circular polarization changed by a factor $\gtrsim 2$ between observing sessions, while any accompanying change in total flux density was $\lesssim 20\%$. Instrumental effects are discussed in some detail. Fluctuations due to system noise provide the main limitation, but for strong sources uncertainties in the determination of the zero of polarization are important.

1. Introduction

Several groups have now reported the detection of small amounts of circular polarization in the emission of a number of extragalactic sources (Biraud and Véron 1968; Biraud 1969; Seaquist 1969*a*, 1971, 1973; Gilbert and Conway 1970; Conway *et al.* 1971; Berge and Seielstad 1972; Roberts *et al.* 1972; Seaquist *et al.* 1973) as well as in the emission from Jupiter's Van Allen belts (Seaquist 1969*b*; Komesaroff *et al.* 1970). In the present paper we report the results of a program in which the Parkes 64 m telescope was used to study the *spectrum* of the circular polarization in relation to the spectrum of the total flux density. Sixty-six sources were observed for circular polarization at one or several of the frequencies 0·63, 1·4, 5·0 and 8·9 GHz, and a subset was then selected for study at all four frequencies.

The degree of circular polarization is so low that special care was required with the observations, and a substantial part of the present paper is devoted to a description of the observing techniques and a discussion of the recognized sources of error (Section 2). The main problems were to achieve adequate sensitivity and to establish the instrumental zero of circular polarization. The instrumental zero was determined from the apparent polarization of HII regions or from the average polarization of many sources. Variations of the zero (on time scales of hours) were monitored by repeated observations of strong sources and by measurements of the receiver unbalance.

The results are presented and briefly discussed in Section 3. In the discussion it is assumed that the circular polarization is the intrinsic polarization of synchrotron emission. Since this component of circular polarization must be present and since it appears to account for the observations, we have not considered alternative origins

for the polarization, such as those discussed by e.g. Pacholczyk and Swihart (1970), Seaquist (1972) and Pacholczyk (1973). Similarly we have not considered it likely that the density of ionized gas would be high enough to modify the synchrotron emission or to produce appreciable free–free absorption (but see e.g. Pacholczyk and Swihart 1973).

Significant circular polarization was found in the emission from 11 extragalactic sources (Table 2 below) as well as from Jupiter. The greatest polarization detected in the extragalactic sources was of the order of $0 \cdot 5 \%$, while the least polarization measured with high significance was $0 \cdot 05 \%$. The total power spectra of 10 of the 11 sources indicate the presence of self-absorbed components, but there is no evidence for a reversal of the sense of polarization in the self-absorbed region, as would be expected for a uniform source. For several sources the circular polarization changed significantly between observing sessions, in agreement with findings by other observers. In some cases the degree of polarization changed by a factor $\gtrsim 2$ while any change in the total intensity was $\lesssim 20 \%$.

The difficulties of estimating magnetic field strengths from the measured degrees of circular polarization are discussed, and a formula is proposed which leads to estimates in the range 10^{-4} to 2×10^{-1} G for the sources studied.

The measurements of Jupiter at $1 \cdot 4$ GHz are consistent with earlier observations, but the circular polarization averaged over a rotation period is nonzero. This is attributed to the relatively large tilt of the axis of rotation relative to the line of sight at the time of the observations. The $5 \cdot 0$ GHz measurements of Jupiter show a much lower degree of circular polarization, and this appears consistent with the dilution by thermal radiation as estimated from linear polarization measurements. Finally, it is noted that measurements for nine of the sources from the first three runs reported here have been given earlier (Roberts *et al.* 1972).

2. Observations and Error Assignment

All the observations were made with the Parkes 64 m telescope. Table 1 gives details for each observing session, namely the observing dates, the polarization system and its characteristics, and the method of establishing the zero point. The runs are identified by the month and year of the observations.

In the column labelled 'Type of feed' in Table 1*b* the symbol TE denotes a smooth cylindrical horn in which a single transverse electric mode is excited, while 1HE and 2HE indicate ridged cylindrical horns in which either one or two hybrid modes are excited (Minnett and Thomas 1966). At both $8 \cdot 9$ and $5 \cdot 0$ GHz the circular polarizations were formed using a quarter-wave plate consisting of a stepped dielectric septum in a circular waveguide. In the $1 \cdot 4$ GHz system (Brooks *et al.* 1971) the two orthogonal linear polarizations were combined in a commercial $90°$ hybrid. For these three frequencies the receiver was switched between the two polarizations by a ferrite switch.

The first $0 \cdot 63$ GHz observations (run 3/72) used the system of Komesaroff *et al.* (1968) in which signals from coplanar crossed dipoles in the end of a feed horn were combined using air-spaced coaxial lines, and diodes were used to switch an extra half-wavelength into one line to reverse the sense of polarization. With such a system there is no direct method of equalizing the losses in the two switch positions. For this reason, in the second $0 \cdot 63$ GHz run (8/72) the linear polarizations were combined

Table 1. Details of observing sessions

(a) Observing dates and basic system parameters

f (GHz)	Observing dates (UT)	Run ident- ifier	Type of receiver[A]	Band- width (MHz)	System temp. (K)	Beam- width ′	Off- set ′	Polar- ization system[B]
0·635	10–13. iii. 72	3/72	P	6	400	32	50	½λ
0·63	7–12.viii.72	8/72	T	80	600	32	50	HD
1·39	18–21. vi. 71	6/71	P	60	250	14	20	HF
1·42	7–10. x. 71	10/71	P	60	400	14	20	HF
1·40	7–13. vii. 72	7/72	P	80	140	14	20–28	HF
1·40	17–22.viii.73	8/73	P	100	150	14	20	HF
5·0	7–9. ix. 71	9/71	CP	300	80	4·4	7	¼λF
5·0	21–25. vi. 72	6/72	CP	300	80	4·4	8	¼λF
8·87	8–11. xi. 71	11/71	CP	30	180	2·6	5	¼λF
8·86	24–28. ii. 72	2/72	CP	35	240	2·7	5	¼λF

(b) Other parameters

Run ident- ifier	Type of feed[C]	Voltage axial ratio[D]	Max. response to linear poln	Zero point — Meth- od[E]	Zero point — Sources used	Zero point — Range (%)	Zero point — Error (%)	RMS error in S_{pol} for 10^3 s on source — Calc. (mJy)	RMS error in S_{pol} for 10^3 s on source — Obs. (mJy)
3/72	TE	0·75	0·11	U	Unpol.[G]	+0·4,+1·2	0·006	12	25
8/72	TE	0·94	0·03	U	Ori A	−0·2,+0·3	0·015	4·8	9
6/71	1HE	0·77	0·13	C	Unpol.[G]	+0·08	0·025	2·0	7
10/71	1HE	0·95	0·04	C	Unpol.[G]	+0·21	0·025	3·7	7
7/72	1HE	0·83	0·18	U	0922–51[H]	+0·08,+0·18	0·005	1·1	3
8/73	1HE	0·81	0·09	U	Unpol.[G]	+0·1,+0·4	0·005	1·1	6
9/71	1HE	0·92	0·04	C	Unpol.[G]	+0·37	0·005	0·4	1·3
6/72	1HE	0·88	0·04	U	RCW 42, 117	−0·16,+0·10	0·005	0·4	1·2
11/71	2HE	Not measured		C	Ori A, M17	−0·01	0·007	3·5	5
2/72[F]	1HE	0·85	0·07	L	HII[I]	−0·06,+0·01	0·013	4·8	9

[A] Abbreviations used are: P, parametric;   T, transistor;   CP, cooled parametric.

[B] Abbreviations used are: ½λ, half-wave switch;   HD, hybrid/diode switch;   HF, hybrid/ferrite switch;   ¼λF, quarter-wave plate/ferrite switch.

[C] Abbreviations used are: TE, excitation of transverse electric mode;   1HE, excitation of one hybrid mode;   2HE, excitation of two hybrid modes.

[D] Mean of two switch positions.

[E] Abbreviations used are: C, zero point assumed const. and equal to mean of all measurements of calibrators;   L, zero point assumed to be linear function of time in each of three consecutive sections of run;   U, zero point assessed from receiver unbalance (see Section 2b).

[F] In this run polarizations measured in phases 1 and 2 differed systematically; means, of course, are used.

[G] All apparently unpolarized sources were used.

[H] HII region RCW 42.

[I] Orion A, RCW 36, 38, 42 and 117, and M17.

in a 90° hybrid and the right-handed (RH) and left-handed (LH) outputs were alternately switched to the receiver using a diode switch.

(a) Observing Procedure

The polarization was switched rapidly (at 39 or ~10 Hz) between LH and RH circular polarization, and the receiver output was synchronously detected. Both this

'switched power' and the 'total power' (sum) were digitally integrated for all on-source and reference measurements. The radiotelescope was directed under computer control to a sequence of positions which alternated between the source position and each of four surrounding reference positions that were offset in the four cardinal directions by the amount indicated in the column labelled 'Offset' in Table 1*a*. Equal time was spent on and off source.

The feed was then rotated by 90° and the sequence of four on–off pairs of measurements were repeated. This rotation served to cancel any response to linear polarization arising because the accepted modes were not circular (as further discussed in subsection (*c*) below). The phase of the switching waveform driving the RF switch was then reversed and the observing sequence repeated, but with the feed orientations in the opposite order. Reversing the phase of the switching voltage provided a convenient means of monitoring the receiver unbalance and thus the instrumental offset of the circular polarization zero (see subsection (*b*) below). The average of the four measurements just outlined (using the two phases of the switching waveform and two orthogonal feed orientations) was counted as one observation.

The pointing of the telescope was checked regularly. This normally ensured that the telescope was directed to within one-tenth of a beamwidth of the direction of maximum response.

The ratio of the receiver gains for the switched and total power signals was monitored by recording, before each source observation, a noise tube calibration which simulated a partially polarized source. This calibration signal, which was injected via a directional coupler following the RF switch, was obtained by combining the output from one end of a noise tube with a small part of the uncorrelated output from the other end. The latter output was switched at the polarization switching frequency. In different runs the 'percentage polarization' of the partially modulated calibration signal was chosen between 2% and 5%.

The sense of polarization was established by measuring the radiation from an LH helical antenna placed at the reflector vertex, and fed by a solid-state noise source. This sense corresponds to RH polarization incident on the reflector. In several observing sessions a cross-check of the sense of polarization was provided by observations of Jupiter, for which the sense of circular polarization as a function of the system III longitude of the central meridian has been established by several observers (Seaquist 1969*b*; Komesaroff *et al.* 1970). The measurements of the helix emission also provided a cross-check on the scale of polarization, since the axial ratio of the helix emission was established in subsidiary observations with the feed set to accept linear polarization. For the first run (6/71) the scale of polarization was in fact established in this way, assuming the helix to have the axial ratio measured in the following 1·4 GHz run (10/71).

(*b*) Zero of Circular Polarization

While the adopted observing procedure reduced many of the instrumental effects, it was found that unpolarized sources still produced a net phase-detected output proportional to the aerial temperature of the source. We term this the 'instrumental circular polarization'. The instrumental polarization was assessed from measurements of radio sources, zero circular polarization being defined either by the polarization of HII regions or by the average polarization of a large number of sources. In the latter case, sources with polarization differing significantly from the mean were

excluded from the average. Table 1*b* indicates which procedure was used for each session and identifies any HII regions used.

Throughout each observing session a few strong sources were observed at frequent intervals to monitor changes in the instrumental polarization; where possible these sources included one or more of the HII regions. In four sessions (identified by C in the column labelled 'Zero point, Method' in Table 1*b*) there was no significant variation of the zero point throughout the run, and the mean of all the calibrator observations was used to define the zero. The run 2/72 was divided into three sections, in each of which the zero point was fitted by a straight-line function of time. In the other five runs (identified by U in the column labelled 'Zero point, Method' in Table 1*b*) the zero point varied by several tenths of 1%, with a strong diurnal component (see example in Fig. 1). No correlation was found with zenith angle: the zero point appeared to be a function of time, probably reflecting changes in the ambient temperature.
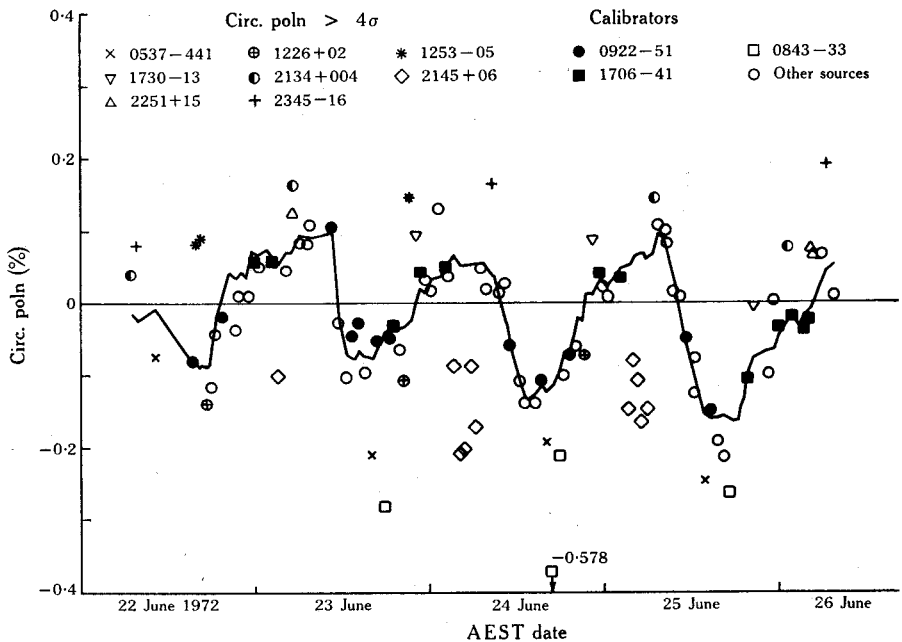

Fig. 1. Measured (uncorrected) circular polarization of sources plotted as a function of time for the 5·0 GHz run 6/72. The line shown is the adopted zero of circular polarization, derived from the measurements of the receiver unbalance as described in the text. Filled symbols are used for calibration sources and other symbols identify sources for which the mean corrected polarization exceeded four times the r.m.s. error, and also the highly linearly polarized source 0843 − 33.

In cases such as that illustrated in Fig. 1 the receiver unbalance was used to establish the zero between measurements of the calibrators. The theory of using the receiver unbalance to monitor the instrumental polarization is due to J. D. Murray (Brooks *et al.* 1971). A small relative fractional loss η in the two channels will cause an instrumental fractional circular polarization of η. If the loss is resistive in components at the ambient temperature T then there will be a differential *emission* equivalent

to an aerial temperature difference of ηT, and this will be detected as an unbalance signal in the switched output.* Besides being used to monitor changes in the zero throughout some runs, this principle was also used to set the instrumental zero at the start of each run. With the telescope directed to 'cold' sky at the zenith, the relative loss in the two channels was adjusted to give zero switched output.
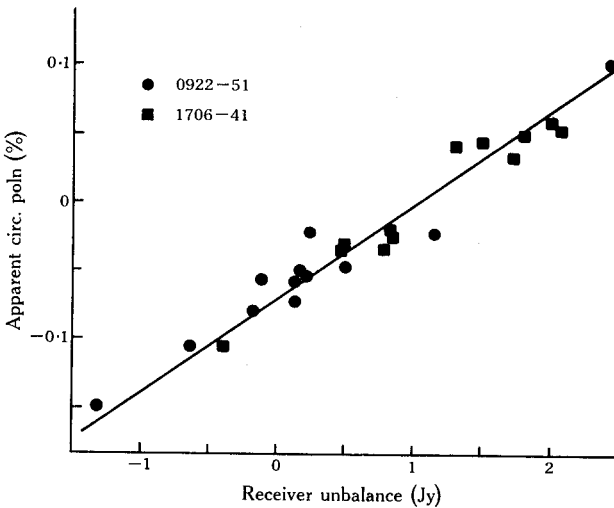

Fig. 2. Apparent circular polarization of the indicated HII region calibration sources as a function of the unbalance of the receiver (converted to equivalent janskys) for the 5·0 GHz run 6/72. The regression line adopted as defining the zero of circular polarization is shown. (Note that 1 Jy = 10^{-26} W m^{-2} Hz^{-1}.)

Fig. 2 shows the measured circular polarization of the calibrators as a function of the receiver unbalance for the observations of Fig. 1. Although this plot does not agree precisely with the simple theory attributed above to J. D. Murray (for example, zero instrumental polarization does not occur at zero unbalance), it is clear that there is a high degree of correlation between the plotted quantities. Hence the zero for each observation was determined from the measured receiver unbalance at the time and the regression line shown in Fig. 2. The zero derived in this way is shown by the line in Fig. 1. For each of the five runs in which this method was used, the slope of the regression line was defined by the 'often observed' sources, while the intercept on the axis was fixed either by the HII region(s) or by the mean of the unpolarized sources (as indicated in the column labelled 'Zero point, Sources used' in Table 1*b*). For four of the five runs, the slope of the regression line was fairly consistent with the theory: the ratio of the actual slope to the theoretical slope ranged from 0·7 (for the case illustrated) to 1·7 (run 8/72). However, for the fifth run treated in this way (7/72) the slope was negative. This is not understood, but since the quantities were highly correlated the regression line was used to define the zero.

* If the loss is reactive it seems that a similar conclusion often applies, but with T now referring to the temperature of a circulator termination.

(c) *Minimizing Response to Linear Polarization*

While the two polarizations accepted by the feeds are elliptical rather than perfectly circular, a considerable degree of ellipticity can be tolerated without appreciable degradation of the sensitivity to circular polarization. For example (see Appendix 2), if the two polarizations accepted have the same voltage axial ratio r but opposite senses, the response to circular polarization is $2r/(1+r^2)$, so that even for r as low as $0 \cdot 5$ there is an 80% response to the circular component.

The more serious effect of the ellipticity is to cause a response to any linear polarization in the incident radiation. This is of particular concern because the linear polarization of radio sources is typically more than 10 times the circular polarization. For cancelling the response to the linear component, we have relied on the procedure of spending equal observing times with the feed in orthogonal orientations. This assumes that rotating the feed through 90° rotates the accepted polarization ellipse through 90° and thus cancels the switched response to linear polarization, as demonstrated in Appendix 3.

(d) *Flux Densities*

Although the observations were not designed to measure flux densities accurately the total power records were used to derive flux densities which are included in Tables 2 and 3 (below). At $8 \cdot 9$ GHz the scale of flux density was based on an assumed (equivalent point source) flux density of 45 Jy for PKS 1228 + 12 (Virgo A). For the other frequencies a scale was established for each run from a weighted mean of observations of those sources for which Harris (1969) gave accurate flux densities. The scale adopted by Harris is such that Hydra A (PKS 0915 − 11) has flux densities of 88, $41 \cdot 3$ and $13 \cdot 0$ Jy at $0 \cdot 63$, $1 \cdot 41$ and $5 \cdot 0$ GHz respectively.

The scatter of the individual measurements of a source in one run yields an r.m.s. error of the mean flux density which is typically ~5%. However, there may well be differences as great as 10% between the scales adopted in different runs at the same nominal frequency. In addition, differences in receiver nonlinearities from run to run could cause further errors of 5%–10%, which are a function of flux density.

(e) *Errors*

For most sources the main contribution to the assessed error of the measured circular polarization was the component determined from the scatter of the observations of a single source. For each run a plot like that shown in Fig. 3 was prepared in which the observed r.m.s. scatter about the mean percentage circular polarization for each source was plotted as a function of the flux density of the source. These plots were quite consistent with the errors for the weaker sources being inversely proportional to the flux density, as would be expected if system noise dominated the error. The implied (constant) error in the measurement of the polarized flux density is listed in the last column of Table 1b together with (in the second last column) the value calculated from the system parameters using the formula (A7) derived in Appendix 1. The observed scatter is consistently larger than the calculated scatter by a factor typically of about two, but in one case as great as five.

In the example shown in Fig. 3 (run 6/72) and in two other runs (7/72 and 8/72) the measured polarizations of the stronger sources (including HII regions) appeared to indicate the presence of an additional component of scatter which did not decrease

with increasing flux density. This perhaps reflects short-term errors in the adopted zero point.

For each observation of a source we have adopted a zero of circular polarization derived from observations of calibrators using one of the methods discussed in subsection (*b*) above. The error in establishing the adopted zero relative to the
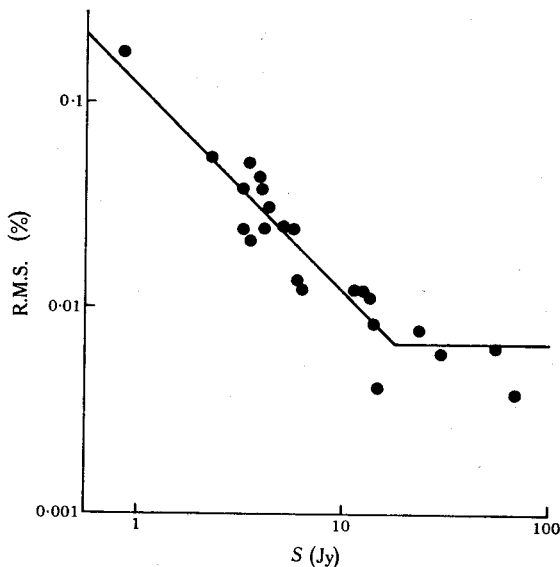

Fig. 3. Plot of the r.m.s. scatter of the corrected values of circular polarization about their mean value (normalized to an on-source time of 10^3 s for each observation) as a function of the flux density of the source. The observations were taken in the 5·0 GHz run 6/72. The lines shown, corresponding to a constant error in polarized flux density for weaker sources and a constant error in percentage polarization for stronger sources, were adopted as minimum values for the scatter component of error.

calibrators was assessed from the deviations δ_i of the observations of the calibrators about the adopted zero. The r.m.s. error of the adopted zero was estimated as

$$\left\{ \sum w_i \delta_i^2 \Big/ \Big((n-m) \sum w_i \Big) \right\}^{\frac{1}{2}}, \qquad (1)$$

where the w_i are weights assigned to the n observations of the calibrator(s) and m is the number of parameters fitted. Any polarization of the (presumed unpolarized) calibrators was estimated for several runs from differences between several HII regions observed, or from differences between HII regions and the average of all those sources whose measured polarizations agreed within twice their r.m.s. scatter (i.e. apparently unpolarized sources). In no case did these different estimates of the zero differ by more than 2·5 times their estimated r.m.s. errors, so that no additional error allowance was made for possible polarization of the calibrators.

Values calculated from the expression (1) are shown in the column labelled 'Zero point, Error' in Table 1*b*, and the errors quoted in Tables 2 and 3 (below) include allowance for this error (except for the calibrators). For the run 2/72, where the zero was fitted with three straight line segments, different errors of the zero were assigned to different segments and the value shown in Table 1*b* is the mean value.

For a few strong, highly polarized sources uncertainties in the scale of polarization contributed appreciably to the total error. The adopted r.m.s. errors of scaling ranged from $0 \cdot 02$ to $0 \cdot 10$ for different runs. Values of $0 \cdot 05$, $0 \cdot 04$ and $0 \cdot 07$ were assigned to the runs 6/71, 9/71 and 10/71 for which Roberts *et al.* (1972) gave an error of $0 \cdot 10$.

Some checks of the off-axis instrumental polarization made at $1 \cdot 4$, $5 \cdot 0$ and $8 \cdot 9$ GHz indicated that errors in circular polarization caused by our pointing inaccuracies ($\leqslant 0 \cdot 1$ beamwidths) would normally be $\leqslant 0 \cdot 017\%$. Because many sources were observed at several different hour angles, these errors should already be included in the scatter component of error. Hence no separate allowance was made for this error. The $8 \cdot 9$ GHz run 2/72 is an exception. It seems likely that the feed used on this occasion was incorrectly assembled, as the off-axis polarization was approximately three times as great as for the other runs. Each observation was therefore assigned an error based on an estimate of the possible pointing error for the particular observation.

Some consideration was also given to the effects of confusion. With an altazimuth-mounted telescope, effects of confusing sources would vary with hour angle. The $0 \cdot 63$ GHz results, which should be those most affected by confusion, were analysed for any hour-angle variations. None were found.

3. Results and Discussion

Circular polarization exceeding four standard deviations was measured for 11 sources (apart from Jupiter). Results for these sources are given in Table 2, and plots of the spectrum of the circular polarization and of the total flux density are given in Figs 4a–4k. For at least eight of these sources, namely PKS 0237 − 23, 0537 − 441, 1127 − 14, 1226 + 02 (3C 273), 1253 − 05 (3C 279), 2134 + 004, 2145 + 06 and 2345 − 16 (Figs 4a–4d, 4f, 4h, 4i and 4k), there seems to be no question of the reality of the measured circular polarization since it is confirmed by detections at several frequencies or in several different observing runs. All eight are identified with quasi-stellar objects. For two other sources, PKS 1730 − 13 (NRAO 530) and 2251 + 15 (3C 454·3), only one measurement exceeds 4σ, but we see no reason to doubt the measurements. For PKS 1228 + 12 (M87) two of the eight measurements are above the 4σ level, but one of them is only a half-measurement made without inversion of the switch phase (run 9/71). This measurement is supported by the measurement in the run 6/72, but both values are so low ($-0 \cdot 029\%$) that they could be affected by uncertainties in the zero of polarization which may not have been properly assessed. Results for the remaining sources are listed in Table 3. For three of the sources in Table 3 polarization exceeding 3σ was measured in one run (only): PKS 0430 + 05 (3C 120), run 2/72; 0624 − 05 (3C 161), run 6/71; and 1934 − 63, run 6/71.

The accuracy of our measurements is attested by their agreement with the Westerbork measurements of similar accuracy (Conway *et al.* 1971), after correction of the sign error in the Westerbork results. They are also in satisfactory agreement with the results of Seaquist *et al.* (1973), and with those of Berge and Seielstad (1972) except in the case of PKS 1226 + 02 (3C 273). Our observations of the latter (Table 2 and Fig. 4d) show the polarization of this source to be remarkably constant at both $5 \cdot 0$ and $8 \cdot 9$ GHz. However, for times shortly prior to and in between our two $5 \cdot 0$ GHz measurements (of $-0 \cdot 066\%$ and $-0 \cdot 068\%$), Berge and Seielstad reported

Table 2.   Sources with detected circular polarization greater than 4σ

Source[A]	| 0·63 GHz | Run identifier	Circ. poln[B] (0·001%)	No. of obs.[C]	S (Jy)	| 1·4 GHz | Run identifier	Circ. poln[B] (0·001%)	No. of obs.[C]	S (Jy)	| 5·0 GHz | Run identifier	Circ. poln[B] (0·001%)	No. of obs.[C]	S (Jy)	| 8·9 GHz | Run identifier	Circ. poln[B] (0·001%)	No. of obs.[C]	S (Jy)
0237−23	3/72	510±120	9	5·5	6/71	311±040	3·5	6·5	9/71	111±025	4	3·3	11/71	−125±190	7	1·9
	8/72	206±080	6	5·1	10/71	448±050	3	7·1	6/72	022±020	5	3·3				
					7/72	243±035	3	6·7								
0537−441	3/72	−1200±700	1	2·7	7/72	−242±035	4	4·9	6/72	−091±016	3	5·4	2/72	−360±075	12	7·5
	8/72	−015±090	5	4·5	8/73	−202±067	3	5·3								
1127−14	3/72	−240±210	3	5·6	6/71	−221±035	3·5	6·1	9/71	−055±015	3·5	6·1	11/71	001±060	7	4·0
	8/72	064±150	5	5·6	10/71	−116±055	5	6·6								
					7/72	−178±028	4	6·7								
1226+02 (3C 273)	3/72	−007±016	6	53	10/71	054±040	2	41	9/71	−066±016	1	50	11/71	−112±017	7	54
	8/72	−029±028	4	53	7/72	−006±015	3	41	6/72	−068[D]±009	3	53	2/72	−124±021	11	57
1228+12 (Virgo A)	3/72	054±020	2	385	10/71	−059±030	1	190	9/71	−029±007	0·5	77	11/71	−017±018	4	45
	8/72	−016±025	4	380	7/72	066±014	4	205	6/72	−029±009	3	69	2/72	−008±015	10	45
1253−05 (3C 279)	3/72	−040±100	2	11·6	6/71	145±030	4	12·5	9/71	060±011	2	14·3	11/71	−028±040	4	11·5
	8/72	110±045	5	11·2	7/72	178±045	5	12·3	6/72	171±009	3	14·9				
1730−13 (NRAO 530)	8/72	213±070	5	5·8	10/71	−036±045	4·5	4·6	6/72	080±015	3	5·0	11/71	106±065	5	4·3
					7/72	068±035	4	4·7								
					8/73	062±079	2	5·5								
2134+004	8/72	419±370	4	1·3	6/71	276±045	5	2·9	9/71	130±014	4	12·7	11/71	044±030	6	12·2
					10/71	429±085	5	3·2	6/72	083±012	4	12·3	2/72	090±060	4	11·6
					7/72	356±050	4	3·0								
2145+06	8/72	−260±200	3	2·6	10/71	−362±120	7	3·2	9/71	−173±025	5	3·9	11/71	−108±070	12	3·5
					7/72	−261±050	4	3·1	6/72	−197±015	11	4·0	2/72	040±210	2	4·8
2251+15 (3C 454·3)					10/71	075±110	1·5	12·0	6/72	066±010	3	14·0	11/71	089±040	2	13·1
					7/72	019±025	2	11·5					2/72	161±045	7	14·6
2345−16	8/72	390±250	4	1·8	10/71	−044±300	3	2·4	9/71	207±045	1·5	3·1	11/71	244±125	5	3·0
					7/72	221±070	3	2·4	6/72	126±025	3	3·2	2/72	195±190	5	3·3

[A] For coordinates see the Parkes catalogue of radio sources (Ekers 1969) or the Parkes 2700 MHz survey (Wall *et al.* 1971; Bolton and Shimmins 1973).

[B] The positive sense is RH about the direction of propagation. The 1σ errors quoted include contributions from all components of error discussed in the text, combined in quadrature.

[C] One observation consists of four measurements: two orthogonal orientations of the feed and two phases of the switching waveform. Measurements (in some of the early runs) made with only one phase of the switching waveform are counted as half observations.

[D] Measured polarization appeared to be a function of hour angle.

$5 \cdot 0$ GHz values ranging from $+0 \cdot 090$ to $+0 \cdot 140$ with individual errors of $1 \cdot 5\sigma$ to 2σ. It might be relevant that in the case of PKS $1253-05$, which is in the same area of the sky, there is a (less significant) disagreement in the same sense, the Berge and Seielstad values again being more positive than ours.

The results presented in Figs $4a$–$4k$ support the conclusion of Gilbert and Conway (1970) that only sources with flat or inverted spectra have detectable circular polarization. However, since the main aim of our program was the study of the spectrum of circular polarization, we selected sources which we hoped might have measurable circular polarization, our main guide being the presence of compact components. Hence only a small number of the sources studied had straight (i.e. power law) spectra, and we cannot use our results for a statistical test.

(a) Relationship of Circular and Linear Polarization

In sources which have a high linear polarization there is presumably a high degree of alignment of the magnetic field. Such sources, *when viewed from a suitable angle*, should also show a high degree of circular polarization. Jupiter is an example of such a source. In an attempt to find other examples we studied two sources with very high degrees of linear polarization: PKS $0843-33$ with a linear polarization of 20% at $5 \cdot 0$ GHz and $1954-55$ with a linear polarization of 17% at $5 \cdot 0$ GHz (Gardner *et al.* 1969). In the case of the latter it is seen from Table 3 that there is no evidence of circular polarization. However, for PKS $0843-33$ (the weakest source in our list) the value measured at $5 \cdot 0$ GHz $(-0 \cdot 230 \pm 0 \cdot 090\%)$ is suggestive of appreciable circular polarization. It is clearly desirable to make further observations of this source to reduce the errors.

The run 8/73 was designed, by one of us (F.B.), to investigate a possible relationship between linear depolarization and circular polarization (Bourret 1973). The sources (apart from calibrators and PKS $0537-441$) were selected at low galactic latitudes where the linear polarization may be considerably reduced by Faraday depolarization. No significant circular polarization was found in any of these sources.

We have also looked for any general correlation between the magnitude of circular and linear polarization, restricting the examination to those measurements with low error. No correlation was evident.

(b) Temporal Variations of Circular Polarization

The circular polarization of both PKS $0237-23$ (Fig. $4a$) and $1253-05$ (3C 279; Fig. $4f$) changed over periods of months. In the case of PKS $0237-23$ the reality of the changes is supported by their systematic variation across the frequency range. Similar variations have been reported for other sources by earlier observers (Biraud and Véron 1968; Biraud 1969; Seaquist 1971, 1973; Berge and Seielstad 1972).

The fractional changes in circular polarization are much greater than any accompanying changes in the total flux density. For example, between September 1971 and June 1972 the circular polarization of PKS $0237-23$ at 5 GHz decreased by a factor of five (or, allowing for errors, by at least a factor of two), while over the same interval the change in the total flux density was less than about 20%. Similar remarks apply to PKS $1253-05$ (3C 279), where over the same interval the circular polarization at 5 GHz increased by a factor of three (or, allowing for errors, by at least a factor of two), while the flux density changed by less than 20%.

S (Jy)

0237−23

4a

Circ. poln (%)

S (Jy)

1127−14

4c

f (GHz)
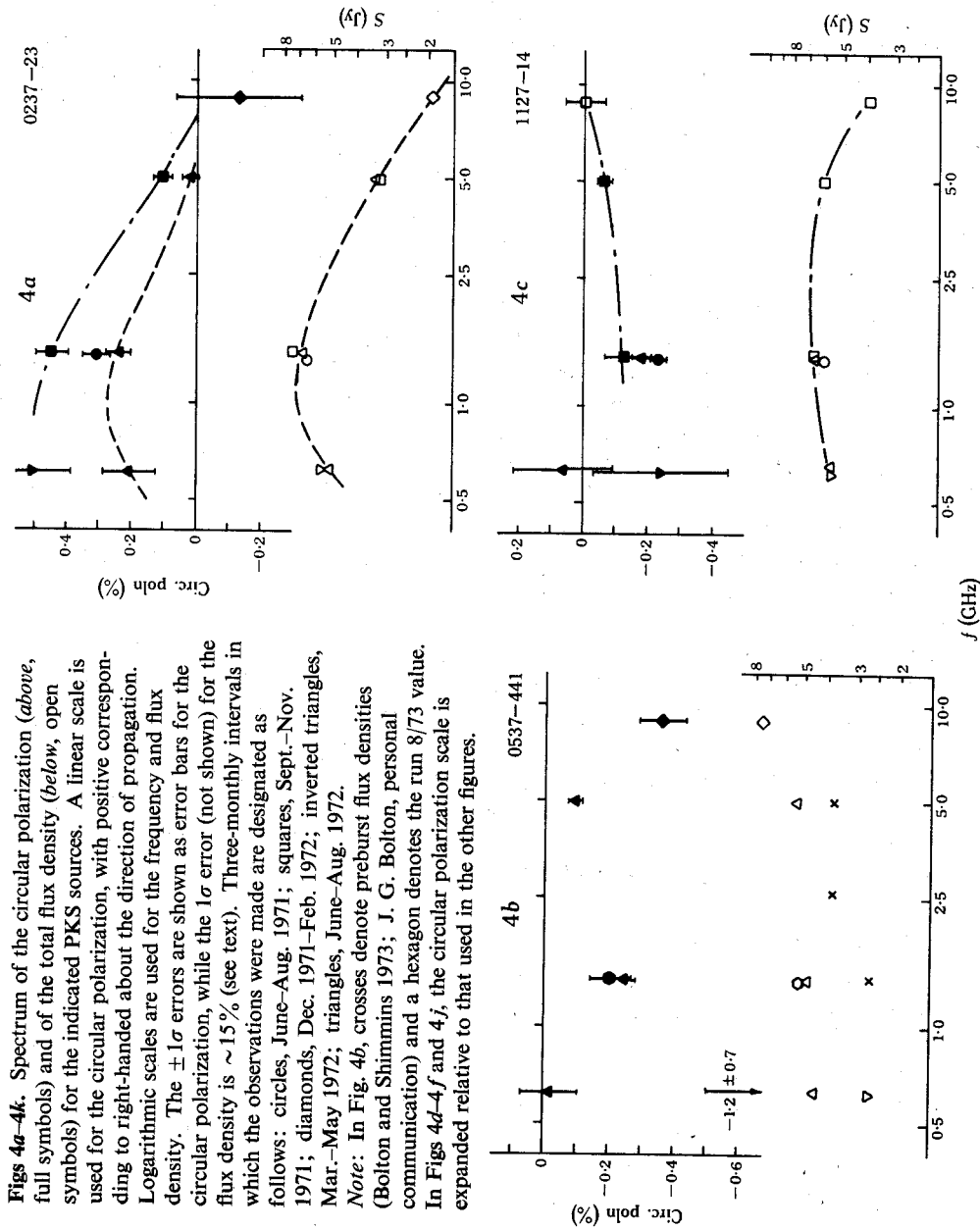
Figs 4a–4k. Spectrum of the circular polarization (*above*, full symbols) and of the total flux density (*below*, open symbols) for the indicated PKS sources. A linear scale is used for the circular polarization, with positive corresponding to right-handed about the direction of propagation. Logarithmic scales are used for the frequency and flux density. The ±1σ errors are shown as error bars for the circular polarization, while the 1σ error (not shown) for the flux density is ~15% (see text). Three-monthly intervals in which the observations were made are designated as follows: circles, June–Aug. 1971; squares, Sept.–Nov. 1971; diamonds, Dec. 1971–Feb. 1972; inverted triangles, Mar.–May 1972; triangles, June–Aug. 1972.

Note: In Fig. 4b, crosses denote preburst flux densities (Bolton and Shimmins 1973; J. G. Bolton, personal communication) and a hexagon denotes the run 8/73 value. In Figs 4d–4f and 4j, the circular polarization scale is expanded relative to that used in the other figures.
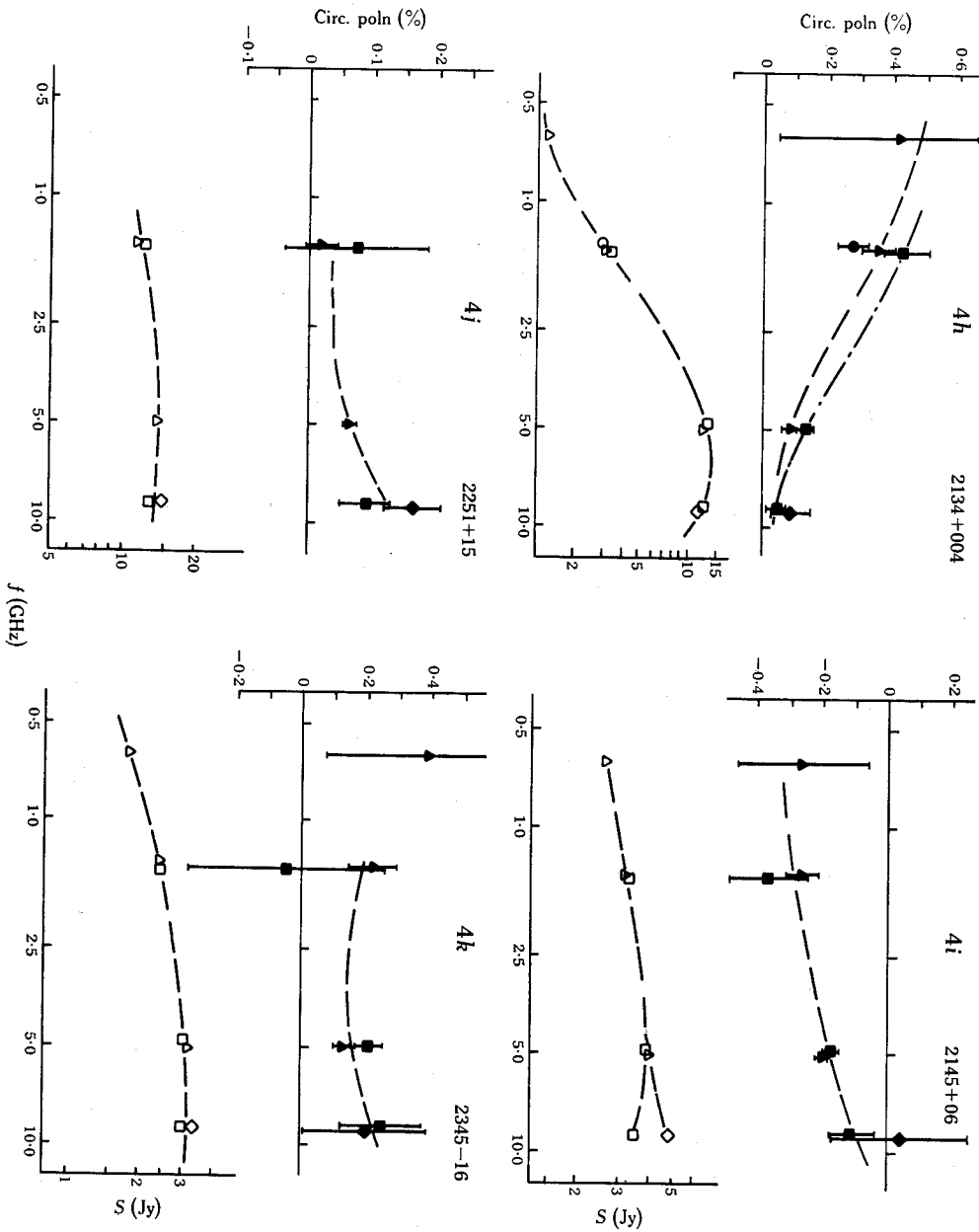
0537−441

4b

Circ. poln (%)

−1·2 ±0·7
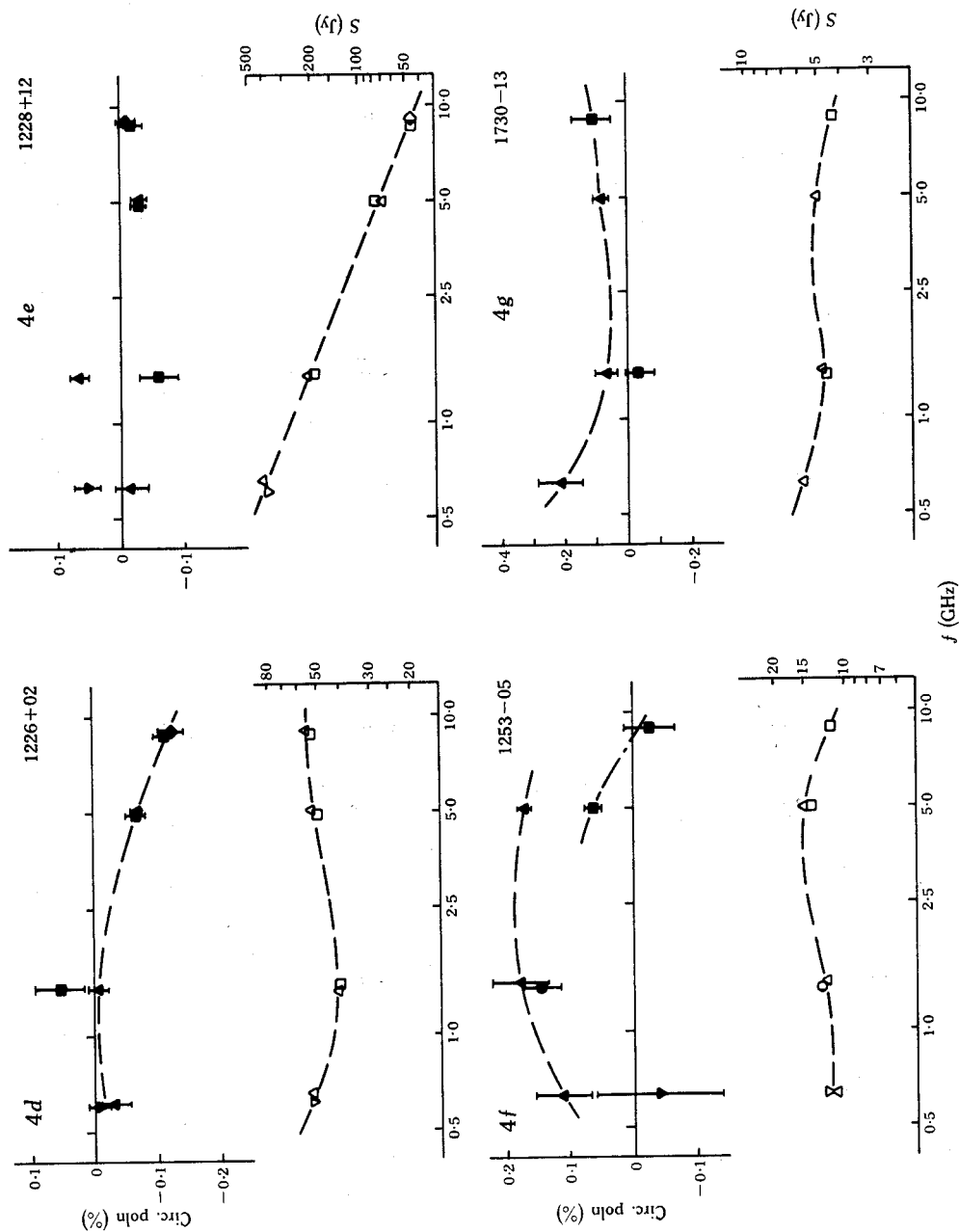
Table 3. Sources with no detected polarization greater than 4σ

Source[A]	Other name	f (GHz)	Run ident.	Circ. poln[B]	No. of obs.[C]	S (Jy)
0003 − 00	3C 2	1·4	8/73	−015 ± 092	2	4·7
0023 − 26		0·63	8/72	024 ± 045	3	13·3
		1·4	6/71	052 ± 035	4	8·3
			10/71	035 ± 030	8·5	8·6
			7/72	−035 ± 025	3	8·3
		5·0	6/72	−023 ± 025	3	3·6
0043 − 42		1·4	7/72	−059 ± 050	2	7·3
0105 − 16	3C 32	1·4	8/73	−045 ± 097	2	4·6
0202 + 14		1·4	6/71	018 ± 150	1	2·8
0316 + 16	CTA 21	1·4	6/71	−119 ± 065	1	6·4
			10/71	−073 ± 040	3	8·1
			7/72	−048 ± 025	4	7·9
		5·0	9/71	−008 ± 040	2	3·1
0410 − 75		0·63	8/72	−008 ± 050	1	24·2
		1·4	6/71	−052 ± 038	1	13·9
			7/72	−012 ± 020	2	13·3
		5·0	6/72	−013 ± 012	6	4·1
0430 + 05	3C 120	1·4	10/71	013 ± 060	4	6·8
		8·9	2/72	170 ± 053	5	11·0
0438 − 43		1·4	10/71	015 ± 075	2·5	7·2
			8/73	−034 ± 057	3	7·6
		5·0	9/71	002 ± 010	5	5·7
0440 − 00	NRAO 190	1·4	6/71	−223 ± 150	1	2·6
			10/71	220 ± 190	3	2·5
0518 + 16	3C 138	0·63	8/72	−009 ± 060	3	13·1
		5·0	6/72	−017 ± 035	2	3·9
0521 − 36		0·63	3/72	060 ± 070	1	28
			8/72	−008 ± 030	2	27
		5·0	9/71	−016 ± 018	2	9·5
		8·9	11/71	006 ± 065	3	6·4
0531 + 19		1·4	8/73	−028 ± 046	3	7·7
0532 − 05	Orion A	0·63	8/72	000	5	260
		8·9	2/72	−005	3	140
0624 − 05	3C 161	0·63	3/72	070 ± 040	10	31
			8/72	−037 ± 025	3	31
		1·4	6/71	−094 ± 029	3	17·6
			10/71	−007 ± 045	5	18·1
			7/72	−014 ± 013	2	18·6
		5·0	9/71	025 ± 023	1·5	6·6
			6/72	−007 ± 016	3	6·3
0625 − 35		1·4	8/73	014 ± 087	2	5·0
0637 − 75		1·4	6/71	−148 ± 085	2	4·9
			10/71	−044 ± 080	3	5·3
0741 − 06		1·4	8/73	091 ± 039	3	9·0
0843 − 33		5·0	6/72	−230 ± 090	4	0·9
0857 − 43	RCW 36	1·4	10/71	−040 ± 030	7·5	25·4
		8·9	11/71	098 ± 040	5·5	11·0
			2/72	022 ± 070	3	13·2
0857 − 47	RCW 38	8·9	2/72	006 ± 020	1	136

Table 3 (*Continued*)

Source[A]	Other name	f (GHz)	Run ident.	Circ. poln[B]	No of obs.[C]	S (Jy)
0915−11	Hydra A	0·63	3/72	009 ± 014	5	88
			8/72	020 ± 020	8	89
		1·4	10/71	055 ± 030	1	41
			7/72	014 ± 014	2	45
		5·0	9/71	018 ± 013	1	13·0
			6/72	−025 ± 013	2	13·8
		8·9	11/71	−044 ± 055	4	6·9
0922−51	RCW 42	1·4	7/72	000	13	30
			8/73	−014	3	34
		5·0	6/72	003	12	23
		8·9	2/72	002 ± 026	9	21
1055+01		1·4	10/71	164 ± 100	3	2·9
1140+22		1·4	8/73	062 ± 104	3	3·4
1144−379		0·63	8/72	−005 ± 340	3	1·9
1151−34		8·9	2/72	160 ± 700	2	2·2
1322−42	Cen A (N)	8·9	11/71	086 ± 045	4	30
	(S)		11/71	−004 ± 060	1·5	20
1328+25·4	3C 287	1·4	8/73	−009 ± 058	2	7·5
1421−49		5·0	9/71	032 ± 021	2	6·0
1504−167		1·4	6/71	173 ± 160	1	2·5
1510−08		1·4	6/71	058 ± 120	1	2·9
			10/71	037 ± 145	4	2·6
1514−24	AP Lib	1·4	6/71	024 ± 075	5	2·0
1549−79		1·4	8/73	−004 ± 067	2	6·6
1648+05	Her A	0·63	3/72	002 ± 020	9	104
			8/72	017 ± 040	2	106
		1·4	10/71	−052 ± 035	2	46
			7/72	−028 ± 015	2	44
		5·0	9/71	−003 ± 015	1	11·3
		8·9	2/72	−005 ± 260	4	5·3
1706−41	RCW 117	5·0	6/72	−003	11	29
		8·9	2/72	−015 ± 044	3	26
1714−37[D]		1·4	10/71	−095 ± 045	2	18·2
		5·0	9/71	007 ± 013	2	9·6
1717−00	3C 353	0·63	8/72	013 ± 040	2	100
		1·4	8/73	−013 ± 012	2	64
1727−21	Kepler's SNR	1·4	10/71	009 ± 035	2	16·1
1814−63		0·63	3/72	−050 ± 090	3	21·6
			8/72	−034 ± 038	2	25·0
		1·4	6/71	007 ± 030	5·5	12·4
			10/71	−003 ± 045	5·5	13·1
			7/72	−035 ± 030	5	12·3
		5·0	9/71	002 ± 012	8	4·4
1817−16	M17	8·9	2/72	004	2	120
1827−36		1·4	8/73	028 ± 051	2	8·6
1830−21[E]		5·0	6/72	−020 ± 020	1	7·3
1921−29	OV −236	8·9	11/71	−021 ± 065	2	6·1
			2/72	−040 ± 066	10	8·2

Table 3 (*Continued*)

Source[A]	Other name	f (GHz)	Run ident.	Circ. poln[B]	No. of obs.[C]	S (Jy)
1932−46		0·63	8/72	−039 ± 036	3	25·6
		1·4	7/72	−029 ± 020	4	11·9
		5·0	6/72	−021 ± 040	3	3·5
1934−63		0·63	3/72	012 ± 045	14	10·6
			8/72	−065 ± 061	3	9·9
	.	1·4	6/71	092 ± 028	3	14·7
			10/71	092 ± 055	2	15·3
			7/72	019 ± 017	3	14·9
		5·0	9/71	005 ± 023	2	5·9
			6/72	−016 ± 016	3	6·1
		8·9	11/71	088 ± 140	5	2·6
1938−15		1·4	8/73	−082 ± 052	2	8·5
1954−55		0·63	8/72	−009 ± 046	3	11·9
		1·4	7/72	034 ± 040	2	6·3
			8/73	−027 ± 057	2	7·6
		5·0	6/72	024 ± 035	4	2·3
2121+24	3C 433	1·4	6/71	077 ± 060	1	12·6
2152−69		0·63	3/72	030 ± 090	4	51
			8/72	−002 ± 017	19	52
		1·4	6/71	003 ± 027	2	29
			7/72	−019 ± 008	17	29
			8/73	022	11	34
		5·0	6/72	−007 ± 011	4	11·5
		8·9	11/71	013 ± 035	10	6·8
2203−18		0·63	3/72	000 ± 700	7	7·5
			8/72	−138 ± 056	5	7·6
		1·4	6/71	119 ± 085	1	6·3
			10/71	030 ± 120	3	6·1
			7/72	−041 ± 025	3	6·5
		5·0	6/72	−018 ± 011	3	4·3
2210+01		1·4	6/71	−042 ± 140	1	2·9
2230+11	CTA 102	0·63	3/72	−480 ± 250	1	7·6
		1·4	10/71	−158 ± 095	2	6·3
			7/72	022 ± 040	2	6·2
		5·0	9/71	−005 ± 028	3	3·5
2331−41		1·4	6/71	054 ± 090	1	4·5
			10/71	−094 ± 160	1	5·0

[A] Apart from 1714−37 and 1830−21 (see notes D and E below), all sources are listed in the Parkes catalogue of radio sources (Shimmins and Day 1968; Ekers 1969) or the Parkes 2700 MHz survey (Bolton and Shimmins 1973).

[B] The positive sense is RH about the direction of propagation. The 1σ errors quoted include contributions from all components of error discussed in the text, combined in quadrature.

[C] One observation consists of four measurements: two orthogonal orientations of the feed and two phases of the switching waveform. Measurements (in some of the early runs) made with only one phase of the switching waveform are counted as half observations.

[D] SNR G349·7+0·2 (Reifenstein *et al.* 1970).

[E] HII(?); 1950·0 coordinates are $18^h 30^m 42^s$, −21°05′·8.

Large changes in the degree of circular polarization with only small changes in the total flux density would occur if the variable component of emission were much more highly polarized than the quiescent emission. For example, a new source component when first generated might have a strong highly ordered magnetic field leading to a relatively large degree of circular polarization, which subsequently decreases. The fact that the highest degree of circular polarization detected at $8 \cdot 9$ GHz occurred in PKS 0537−441 after a substantial enhancement in flux density (Peterson and Bolton 1972) lends support to this explanation. In an address given at the 15th General Assembly of the I.A.U., Sydney, 1973, G. A. Seielstad suggested another possible explanation, namely a change in the mean angle between the observer's line of sight and the direction of the magnetic field. He pointed out that this effect is known to occur in the case of Jupiter.

(c) Spectrum of Circular Polarization

The variability of the circular polarization complicates the measurement of its spectrum, but our observations seem to be sufficiently closely spaced in time to define the main trends. In Figs 4a–4k, where large variations occurred between runs, separate curves have been sketched through observations obtained within the same three-month interval. With the possible exception of PKS 1228+12 (M87), for which the measured polarization is very low, there is no evidence for a reversal of the sense of polarization across the frequency range studied (see Figs 4a–4k). For most of the sources, the points from all the runs have the same sign, while, where there are points of opposite sign, these have relatively large errors. For a *uniform* synchrotron emitting source, a reversal of the sense of circular polarization is predicted to occur at a frequency where the source is becoming optically thick (Ramaty 1969; Melrose 1971, 1972; Pacholczyk and Swihart 1971b). Because of an error in sign of the published results of Conway *et al.* (1971) it was at one time thought there was evidence for this effect (Pacholczyk and Swihart 1971a). However, our observations show no evidence for the effect even for sources, such as PKS 0237−23 and 2134+004, whose spectra approximate most closely to that of a uniform source.

There is a general tendency for the degree of circular polarization to increase as the frequency decreases, in several cases more rapidly than proportionally to $f^{-0 \cdot 5}$ as predicted by the simple theory. Only in one case is there clear evidence of a decrease with decreasing frequency, namely in the case of PKS 1226+02 (3C 273; Fig. 4d). Conway *et al.* (1971) interpreted their observations as suggesting 'that sources may show circular polarization at wavelengths at which they are opaque, but do not do so at wavelengths at which they are transparent'. Our observations of PKS 0237−23 (Fig. 4a) certainly do not support this conclusion.

We think the disagreement between these observations and the theory for a uniform source will probably be resolved when the theory of nonuniform sources is developed. As a step in this direction two of us (R.S.R. and J.A.R.), using formulae from Melrose (1972) and with the programming assistance of Henrietta May, developed an interactive computer program which displayed the spectrum of polarization and flux density for a model consisting of up to three uniform components. The observational results were also displayed and, by trial-and-error adjustment of the peak total flux density, the peak frequency, and the peak degree of circular polarization of each component, we found that we could obtain quite satisfactory fits to the data.

While this modelling is rather crude it does demonstrate that the observations can be fitted by synchrotron models with more complex geometry. Furthermore, since it is known from very long baseline interferometry (VLBI) observations that many of the sources in Table 2 in fact consist of several components, the components we have fitted may have some reality. For this reason, in discussing magnetic field strengths in subsection (e) below, we consider the field strengths inferred for these components.
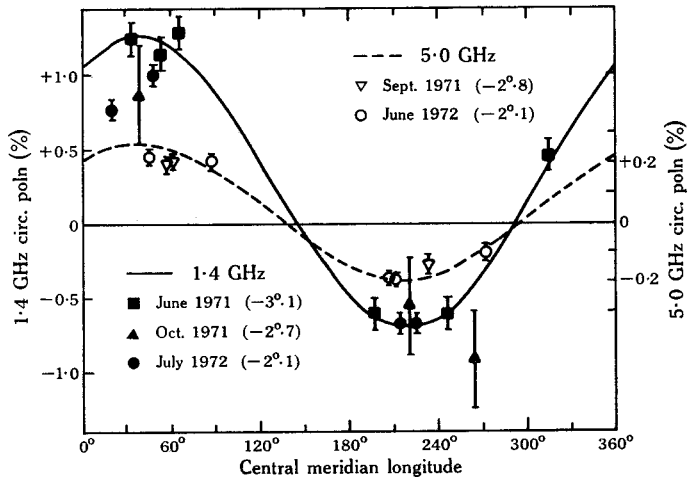

Fig. 5. Circular polarization of Jupiter at $1 \cdot 4$ GHz (full symbols and curve; refer to left-hand axis) and $5 \cdot 0$ GHz (open symbols and dashed curve; refer to right-hand axis) plotted as a function of the modified system III longitude of the central meridian. This system agrees with the IAU system III at $1972 \cdot 0$ (see text). Values of D_E are included in the legends defining the symbols. The curves are sinusoids of the phase indicated by the observations of Biraud *et al.* (see text). The $1 \cdot 4$ GHz curve has an amplitude of $0 \cdot 99\%$ and mean value of $0 \cdot 28\%$. The $5 \cdot 0$ GHz curve has an amplitude of $0 \cdot 23\%$ and mean value of $0 \cdot 04\%$.

In this model fitting, the circular polarization could be made to continue to increase down to frequencies well below the maximum of the total intensity simply by assigning a high degree of circular polarization to the component peaking at a low frequency. The reversal of the sense of polarization at low frequencies was not prevented but was postponed to a lower frequency. Since the completion of this investigation, Robinson (1974) has investigated the circular polarization of a class of source in which the magnetic field is nonuniform. For these sources there is no reversal of the sense of polarization but the degree of polarization drops to a low value in the optically thick regime. A model consisting of several such components could clearly also be made to fit the observations, but at present there would be insufficient observations to define the parameters of this more complicated model.

(d) Jupiter

In the present series of observations no attempt was made to study the circular polarization of Jupiter throughout its rotational period (but see a forthcoming publication by Biraud *et al.* reporting observations made in August 1973). However, in several runs, observations were made at times when the polarization was near a

maximum of one sense or the other. These measurements are plotted in Fig. 5. To allow for the slight difference between the true rotational period and the IAU system III period, a modified system III longitude is used defined by

$$l_{\text{III}} = l_{\text{III}}(\text{IAU}) - 3°{\cdot}2(y - 1972{\cdot}0),$$

where y is the epoch of observation expressed in decimal years. This longitude system agrees with the IAU system at 1972·0, and the corrections applied in no case amounted to more than 2°.

The 1·4 GHz observations (solid symbols in Fig. 5) show a total range of circular polarization of close to 2%, in conformity with the findings of Seaquist (1969b) and Komesaroff *et al.* (1970). However, the mean polarization is clearly not zero. This presumably arises from the tilt of the axis of rotation of the planet relative to the plane of the sky at the time of these observations. Both the sense and magnitude of the difference are consistent with the values of this tilt, which ranged from $-2°{\cdot}1$ to $-3°{\cdot}1$ at the time of the observations. (This tilt is equal to D_{E}, the declination of the Earth as seen from Jupiter; see caption to Fig. 5.)

The 5·0 GHz measurements are the first reported observations of the circular polarization of Jupiter at a frequency as high as this. The degree of circular polarization is considerably less than that at 1·4 GHz, the ratio of the amplitudes of the two curves in Fig. 5 being 0·23. The factor $f^{-0{\cdot}5}$ in the expression for the circular polarization of optically thin synchrotron emission (equation (2) below) would account for a drop by a factor of 0·53. The remaining factor of 0·43 presumably arises from dilution by thermal emission. The fraction of the 5·0 GHz emission which is synchrotron emission is not well established, but this factor of 0·43 is in reasonable agreement with an estimate based on the degree of *linear* polarization. Thus, if it is assumed that the peak linear polarization of the synchrotron component is the same at 5·0 GHz as at 1·4 GHz, then the ratio of the 8·5% linear polarization observed at 5·0 GHz (Whiteoak *et al.* 1969) to the 22% observed at 1·4 GHz (Roberts and Komesaroff 1965) yields a ratio of synchrotron to total 5·0 GHz emission of 0·38. In view of the errors, this is in quite satisfactory accord with the factor of 0·43 estimated from the circular polarization. (The corresponding thermal disc temperature is about 200 K.)

(e) Deduced Magnetic Field Strengths in Sources

In principle, a measurement of the circular polarization of a synchrotron emitting source provides a measurement of the magnetic field strength in the source. However, in practice there are several difficulties. Consider a uniform optically thin source in which the electrons have a differential distribution of pitch angles proportional to $\sin^q \alpha$ (α being the pitch angle and q a constant), and a differential distribution of energies E proportional to E^{-2} (leading to an $f^{-0{\cdot}5}$ spectrum). Then from the theory of Legg and Westfold (1968) it may be shown that the degree of circular polarization m_c is given by

$$m_c = 1{\cdot}64(1 + \tfrac{1}{4}q)(\cos\theta/\sin^{\frac{1}{2}}\theta)(f_B/f)^{\frac{1}{2}}. \tag{2}$$

Here θ is the angle between the direction of the magnetic field and the direction of

the observer, f is the frequency of observation and f_B is the nonrelativistic gyro-frequency, related to the magnetic field strength B by the formula

$$f_B = eB/2\pi m.$$

Inverting equation (2) we have

$$B = \frac{1\cdot3\times10^{-2}}{(1+\frac{1}{4}q)^2}\frac{\sin\theta}{\cos^2\theta}fm_c^2, \tag{3}$$

where B is in gauss, f in gigahertz and m_c in per cent.

Before we use such a formula to deduce a magnetic field strength B from a measured degree of circular polarization m_c, not only must we insert appropriate values for the orientation θ of the magnetic field and for the pitch angle parameter q but we must consider the effects of the nonuniformity of the source and the effects of synchrotron self-absorption. A method of effectively selecting a mean value for θ is to replace equation (2) by the expression for the r.m.s. value of m_c averaged over all directions of viewing (all θ). This is found to be

$$\langle m_c^2\rangle^{\frac{1}{2}} = 1\cdot28(1+\frac{1}{4}q)(f_B/f)^{\frac{1}{2}}. \tag{4}$$

(The corresponding *mean* value of m_c is, of course, zero.) It is customary to assume an isotropic pitch angle distribution ($q = 0$). To allow for the partial cancellation arising from differences in the field directions in different parts of a nonuniform source, Rosenberg (1972) has suggested reducing equation (4) by the mean factor by which the integrated *linear* polarization of sources is found to lie below the value predicted for uniform sources. He assessed this as 1/14. However, the sources in which circular polarization has been detected to date are, by observational selection, among the most highly circularly polarized. It therefore seems appropriate that a 'disorder factor' assessed from the integrated linear polarization of sources should be based, not on the average, but on the highest integrated linear polarizations that are observed. As these are about 20% while the polarization predicted for a uniform region is about 70%, this leads to a disorder factor of only $0\cdot3$.

If this factor is incorporated into equation (4), with $q = 0$, and the equation is then inverted, the following expression for B is obtained:

$$B = 0\cdot2fm_c^2 \tag{5}$$

(B in gauss, f in gigahertz and m_c in per cent). We adopt this equation as a means of estimating magnetic field strengths, but it is clear that values deduced from this formula should be regarded as order-of-magnitude estimates only. No allowance has been made for self-absorption, since the peak values of circular polarization are not much affected by the absorption. But if several components are present the value used for m_c should refer to the particular component considered.

Equation (5) was used to deduce field strengths in all the sources for which significant circular polarization was measured. For measurements at $1\cdot4$ and $5\cdot0$ GHz the deduced field strengths range from about 10^{-4} to 6×10^{-2} G, with a median value $\sim10^{-3}$ G. Values inferred from the $8\cdot9$ GHz measurements (only four in number) tend to be higher, ranging from 2×10^{-2} to 2×10^{-1} G. This perhaps

reflects the fact that more compact components dominate the 8·9 GHz emission. The lack of high polarizations at 0·63 GHz likewise probably arises from the smallness of the contribution of compact components at this frequency.

In passing, it is of interest to apply the formula (5) to the case of Jupiter. The measured 1% circular polarization at 1·4 GHz would, according to this formula, imply a value of $B \approx 0·3$ G, which is quite close to the value measured by Pioneer 10 (0·19 G; Smith *et al.* 1974). The agreement is largely fortuitous; Jupiter happens to have an unfavourable orientation ($\theta = 80°$) and a very high degree of order, while some 30% of the electrons are in very flat helices, i.e. have a large value of q.

For optically thick components, for which angular sizes are available, an independent estimate of the magnetic field strength can be made from the brightness. For several of the sources for which we have measured circular polarization there is VLBI information on the angular sizes. We have attempted to identify the components that we fitted to the spectra (subsection (*c*) above) with the components derived from the angular size measurements, and then compared the magnetic field strength deduced from the optically thick brightness and from the circular polarization. As Seaquist (1973) has emphasized, such comparisons provide a check on the synchrotron origin of the circular polarization. Alternatively, if this origin is accepted, these comparisons can provide information on the mean angle θ to the magnetic field and on the pitch angle distribution.

Our comparisons revealed no glaring inconsistencies, but it appears that at present the data are insufficient for very meaningful comparisons to be made. Because the magnetic field strength derived from the optically thick brightness depends on the *square* of the brightness, it is necessary to measure the angular size accurately and in both dimensions. Likewise it is necessary to apportion correctly the contributions of the different components to the total intensity and to the net circular polarization. This requires measurements of the circular polarization with low error at several frequencies. Furthermore, all of the observations, both of angular size and of polarization, must be made within a time interval sufficiently short that significant variations have not occurred. It seems that at present these conditions have not been satisfied, but that a concentrated study of several of the sources might be profitable.

4. Conclusions

By adding the sources PKS 0237−23, 0537−441, 1226+02 (3C 273), 2134+004, 2145+06 and 2345−16 to the list of extragalactic sources definitely known to be circularly polarized, this investigation has doubled the number of such sources. Studies of these sources over a 14:1 frequency range have provided information on the spectrum of circular polarization, and its variability. However, the program has also highlighted the need for technical improvements before studies of circular polarization are likely to be very rewarding. We conclude with some discussion of these problems.

The first need is for higher sensitivity, and we mention four possible improvements:

(i) Lower system temperatures. The present systems do not reach the confusion limit for circular polarization.

(ii) Dual-channel systems performing continuous differencing. This would achieve a factor-of-$\sqrt{2}$ improvement.

(iii) An observing technique that does not require the off-source observations. This would provide a factor-of-2 improvement.

(iv) Achievement of the theoretical possibilities of the present systems, leading to a factor-of-$\geqslant 2$ improvement (see Table 1*b*).

Because the circular polarization of many sources changes with time, observations are needed at intervals of a few months at each of several frequencies. The requirement for high sensitivity effectively limits the observations to instruments of large collecting area so that the scheduling of such observations is difficult.

The second need is to stabilize the instrumental zero of circular polarization, which presumably requires temperature control of elements at the focus. It is also necessary to develop better means of measuring the zero point. We have given some consideration to the construction of a radiator with zero circular polarization to be mounted at the paraboloid vertex. This poses some interesting problems: whereas zero linear polarization can be established from the mean of emissions from the same radiator in two orthogonal orientations, the corresponding procedure for circular polarization, requiring viewing the radiator from front and rear, is difficult to achieve.

Finally we mention the problem of extended sources. In the 8·9 GHz sessions of the present program an attempt was made to study the circular polarization of the Crab Nebula, mainly to test the predictions of Rees (1971). However, insufficient time was available for adequate calibration of the off-axis instrumental effects, and we could not be confident of the results. Perhaps extended sources are more simply studied by synthesis techniques where the primary beams of the telescopes can be much larger than the object studied.

Acknowledgments

References

Berge, G. L., and Seielstad, G. A. (1972). *Astron. J.* **77**, 810.
Biraud, F. (1969). *Astron. Astrophys.* **1**, 156.
Biraud, F., and Véron, P. (1968). *Nature (London)* **219**, 254.
Bolton, J. G., and Shimmins, A. J. (1973). *Aust. J. Phys. Astrophys. Suppl.* No. 30.
Bourret, R. (1973). *Astrophys. Space Sci.* **24**, 407.
Brooks, J. W., Murray, J. D., and Radhakrishnan, V. (1971). *Astrophys. Lett.* **8**, 121.
Conway, R. G., Gilbert, J. A., Raimond, E., and Weiller, K. W. (1971). *Mon. Notic. Roy. Astron. Soc.* **152**, 1P.
Ekers, Jennifer A. (Ed.) (1969). *Aust. J. Phys. Astrophys. Suppl.* No. 7.
Gardner, F. F., Whiteoak, J. B., and Morris, D. (1969). *Aust. J. Phys.* **22**, 821.
Gilbert, J. A., and Conway, R. G. (1970). *Nature (London)* **227**, 585.
Harris, Beverley J. (1969). Ph.D. Thesis, Australian National University.

Komesaroff, M. M., Gardner, F. F., Morris, D., Roberts, J. A., and Whiteoak, J. B. (1968). *Nature (London)* **218**, 73.

Komesaroff, M. M., Morris, D., and Roberts, J. A. (1970). *Astrophys. Lett.* **7**, 31.

Legg, M. P. C., and Westfold, K. C. (1968). *Astrophys. J.* **154**, 499.

Melrose, D. B. (1971). *Astrophys. Space Sci.* **12**, 172.

Melrose, D. B. (1972). *Proc. Astron. Soc. Aust.* **2**, 140.

Minnett, H. C., and Thomas, B. MacA. (1966). *IEEE Trans. Antennas Propagat.* AP **14**, 654.

Pacholczyk, A. G. (1973). *Mon. Notic. Roy. Astron. Soc.* **163**, 29P.

Pacholczyk, A. G., and Swihart, T. L. (1970). *Astrophys. J.* **161**, 415.

Pacholczyk, A. G., and Swihart, T. L. (1971*a*). *Mon. Notic. Roy. Astron. Soc.* **153**, 3P.

Pacholczyk, A. G., and Swihart, T. L. (1971*b*). *Astrophys. J.* **170**, 405.

Pacholczyk, A. G., and Swihart, T. L. (1973). *Astrophys. J.* **179**, 21.

Pancharatnam, S. (1956). *Proc. Indian Acad. Sci.* A **44**, 247.

Peterson, B. A., and Bolton, J. G. (1972). *Astrophys. Lett.* **10**, 105.

Ramaty, R. (1969). *Astrophys. J.* **158**, 753.

Rees, M. J. (1971). *Nature (London) Phys. Sci.* **230**, 55.

Reifenstein, E. C., III, Wilson, T. L., Burke, B. F., Mezger, P. G., and Altenhoff, W. J. (1970). *Astron. Astrophys.* **4**, 357.

Roberts, J. A., and Komesaroff, M. M. (1965). *Icarus.* **4**, 127.

Roberts, J. A., Ribes, J.-C., Murray, J. D., and Cooke, D. J. (1972). *Nature (London) Phys. Sci.* **236**, 3.

Robinson, R. D. (1974). *Proc. Astron. Soc. Aust.* **2**, 258.

Rosenberg, H. (1972). *Astron. Astrophys.* **19**, 66.

Seaquist, E. R. (1969*a*). *Astrophys. Lett.* **5**, 111.

Seaquist, E. R. (1969*b*). *Nature (London)* **224**, 1011.

Seaquist, E. R. (1971). *Nature (London) Phys. Sci.* **231**, 93.

Seaquist, E. R. (1972). *Astrophys. Space Sci.* **15**, 284.

Seaquist, E. R. (1973). *Astron. Astrophys.* **22**, 299.

Seaquist, E. R., Gregory, P. C., Biraud, F., and Clark, T. R. (1973). *Nature (London) Phys. Sci.* **242**, 20.

Shimmins, A. J., and Day, G. A. (1968). *Aust. J. Phys.* **21**, 377.

Smith, E. J., *et al.* (1974). *Science* **183**, 305.

Wall, J. V., Shimmins, A. J., and Merkelijn, J. K. (1971). *Aust. J. Phys. Astrophys. Suppl.* No. 19.

Whiteoak, J. B., Gardner, F. F., and Morris, D. (1969). *Astrophys. Lett.* **3**, 81.

Appendix 1. Circular Polarization Error

In this appendix we derive a formula for the error that arises in the measured circular polarization solely from system noise errors in the switched power. A source with flux density S_p in the polarization accepted by the aerial produces an aerial temperature

$$T_a = (A_e/k)S_p, \tag{A1}$$

where A_e is the effective area of the antenna for this polarization and k is Boltzmann's constant. Note the factor-of-2 difference from the 'usual' formula for the aerial temperature produced by an *unpolarized* source of *total* flux density S, namely

$$T_a = (A_e/2k)S. \tag{A2}$$

When a source with RH polarized flux density S_R and LH polarized flux density S_L is observed with the switched system, the aerial temperatures in the two switch positions are

$$T_R = (A_e/k)S_R + T_{sR} \qquad \text{and} \qquad T_L = (A_e/k)S_L + T_{sL}. \tag{A3}$$

Here T_{sR} and T_{sL} are the system temperatures in the two polarizations (including contributions of ground and sky), and we have assumed that the effective area is the same in the RH and LH modes. If we suppose that the noise bandwidth is Δf (MHz), and that a time t (s) is spent integrating on source and an equal time off source, then T_R on source is measured in a time $\frac{1}{2}t$ and consequently the r.m.s. error in the measurement of T_R is (since Δf is in MHz)

$$10^{-3} T_s (\tfrac{1}{2} t \Delta f)^{-\frac{1}{2}}, \tag{A4}$$

where we have written $T_{sR} \approx T_{sL} \approx T_s$. Since T_L on source is measured with the same error, $T_R - T_L$ on source is measured with an error of

$$2 \times 10^{-3} T_s (t \Delta f)^{-\frac{1}{2}}. \tag{A5}$$

Off source, $T_R - T_L$ is measured with the same error, so that $T_R - T_L$ on source minus $T_R - T_L$ off source is measured with an r.m.s. error of

$$2^{3/2} \times 10^{-3} T_s (t \Delta f)^{-\frac{1}{2}}. \tag{A6}$$

Consequently the polarized flux density $S_R - S_L$ is measured with an error of

$$\sqrt{2} \times 10^{-3} (2k/A_e) T_s (t \Delta f)^{-\frac{1}{2}}, \tag{A7}$$

which we have written so that the first bracketed term is the factor relating *total* flux density to aerial temperature in the 'usual' expression (A2). Values of $(2k/A_e)$ for the Parkes 64 m reflector are (D. E. Yabsley, personal communication):

f	0·63	1·4	5·0	8·9	8·9	GHz
Feed	TE	1HE	1HE	2HE	1HE	
$2k/A_e$	1·59	1·60	1·86	2·28	2·64	Jy K^{-1}

Appendix 2. Response to Circular Polarization

In this appendix we consider the response to circular polarization of a switched elliptically polarized receiver. For this purpose we refer to the representation of the Poincaré sphere shown in Fig. 6. The poles RC and LC denote right-handed and left-handed circular polarization, while various directions of linear polarization are represented by points on the equator. We suppose that the incident circular polarization is RC and that the elliptical polarization accepted in one switch position is represented by the point E. The voltage axial ratio of the accepted polarization ellipse is then

$$r = \tan \chi, \tag{A8}$$

where the angle 2χ is defined in Fig. 6. We make use of the theorem (see e.g. Pancharatnam 1956) that the fraction of the power accepted is given by the square of the cosine of half the angle at the centre of the sphere subtended by the arc which joins the points representing the incident and accepted polarizations. Thus the fraction of the power accepted is $\cos^2 \alpha$.

In the other switch position, we suppose that the accepted polarization (represented by point E′) has the opposite sense, has arbitrary relative orientation of the major axis, and has an axial ratio given by

$$r' = \tan \chi' = \tan(45° - \alpha').$$

The fraction of the incident RC power accepted will be $\cos^2(90° - \alpha')$, and the response of a differencing* system will be

$$\cos^2 \alpha - \sin^2 \alpha'.$$

In the special case where the axial ratios in the two opposite switch positions are equal this becomes

$$\cos 2\alpha = \sin 2\chi.$$

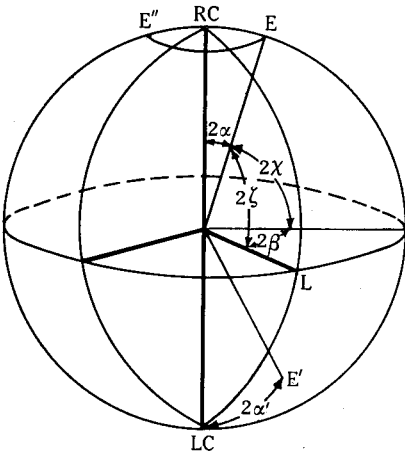or, in view of equation (A8),

$$2r/(1+r^2). \tag{A9}$$

Fig. 6. Representation of the Poincaré sphere. The poles RC and LC correspond to right-handed and left-handed circular polarization respectively. Various directions of linear polarization are represented around the equator.

Appendix 3. Cancellation of Response to Linear Polarization

In this appendix we examine the cancellation of the response to linear polarization that occurs when a switched elliptically polarized receiving system is used in two orthogonal orientations. Let E and E′ (Fig. 6) again denote the accepted elliptical polarizations in the two switch positions, and let L denote the incident linear polarization. In switch position 1 the fraction of the power accepted is then

$$\cos^2 \zeta = \tfrac{1}{2}(1 + \cos 2\zeta) = \tfrac{1}{2}(1 + \cos 2\chi \cos 2\beta).$$

In the other switch position the fraction accepted is

$$\tfrac{1}{2}(1 + \cos 2\chi' \cos 2\beta'),$$

* For a 'switched' system there is an additional factor of $\tfrac{1}{2}$ because each polarization is accepted for only half the time.

where the primed angles are the corresponding angles for E′. The difference is thus

$$\tfrac{1}{2}(\cos 2\chi \cos 2\beta - \cos 2\chi' \cos 2\beta') . \tag{A10}$$

A rotation of the accepted polarization ellipse through 90° corresponds to a rotation of the point on the Poincaré sphere through 180°, i.e. from E to E″. In this condition the fraction of the power accepted in switch position 1 is

$$\tfrac{1}{2}\{1 + \cos 2\chi \cos(180° - 2\beta)\} ,$$

and the difference between the fractions accepted in the two switch positions is

$$\tfrac{1}{2}\{\cos 2\chi \cos(180° - 2\beta) - \cos 2\chi' \cos(180° - 2\beta')\} . \tag{A11}$$

The average of (A10) and (A11) is zero.